RSC Advances

PAPER

View Article Online
View Journal | View Issue

Cite this: *RSC Adv.*, 2018, **8**, 2219

G_s protein peptidomimetics as allosteric modulators of the β_2-adrenergic receptor†

Lotte-Emilie Boyhus,[a] Mia Danielsen,[a] Nina Smidt Bengtson,[a] Micha Ben Achim Kunze,[b] Xavier Kubiak,[c] Tjerk J. Sminia,[a] Jacob Hartvig Løper,[a] Phuong Thu Tran,[a] Kresten Lindorff-Larsen,[b] Søren G. F. Rasmussen,[c] Jesper Mosolff Mathiesen‡*[a] and Daniel Sejer Pedersen‡*[a]

A series of G_s protein peptidomimetics were designed and synthesised based on the published X-ray crystal structure of the active state β_2-adrenergic receptor (β_2AR) in complex with the G_s protein (PDB 3SN6). We hypothesised that such peptidomimetics may function as allosteric modulators that target the intracellular G_s protein binding site of the β_2AR. Peptidomimetics were designed to mimic the 15 residue C-terminal α-helix of the G_s protein and were pre-organised in a helical conformation by (*i*, *i* + 4)-stapling using copper catalysed azide alkyne cycloaddition. Linear and stapled peptidomimetics were analysed by circular dichroism (CD) and characterised in a membrane-based cAMP accumulation assay and in a bimane fluorescence assay on purified β_2AR. Several peptidomimetics inhibited agonist isoproterenol (ISO) induced cAMP formation by lowering the ISO maximal efficacy up to 61%. Moreover, some peptidomimetics were found to significantly decrease the potency of ISO up to 39-fold. In the bimane fluorescence assay none of the tested peptidomimetics could stabilise an active-like conformation of β_2AR. Overall, the obtained pharmacological data suggest that some of the peptidomimetics may be able to compete with the native G_s protein for the intracellular binding site to block ISO-induced cAMP formation, but are unable to stabilise an active-like receptor conformation.

Received 23rd October 2017
Accepted 4th December 2017

DOI: 10.1039/c7ra11713b

rsc.li/rsc-advances

Introduction

The importance of G protein-coupled receptors (GPCRs) within drug discovery is undisputed. It is estimated that >25% of FDA approved drugs act *via* GPCRs.[1] However, only 27% of non-olfactory GPCRs are currently targeted by an approved drug and 15% are currently in clinical trials, leaving 232 non-olfactory GPCRs that remain entirely unexploited as drug targets.[2] Despite the central importance of GPCRs, we still have a very rudimentary understanding of the structure and function of this family of membrane-spanning receptors, particularly with respect to how GPCRs interact with intracellular proteins to achieve signal transduction and physiological responses. GPCR ligands generally bind to the extracellular side of the receptor and target the orthosteric or allosteric binding sites, or both as bivalent ligands.[3] On the other hand, the intracellular surface of GPCRs has largely been ignored in the development of allosteric modulators. Such allosteric modulators could conceivably be designed to target the receptor surface responsible for recruiting intracellular transducers such as the G proteins and arrestins and thus be useful pharmacological tool compounds for studying GPCR signal transduction and possibly provide a new avenue for drug discovery. Moreover, such compounds could be useful compounds for X-ray crystallography to stabilise GPCRs in their active state conformation, which is particularly difficult to crystallise due to the high degree of receptor flexibility in the receptor active state. Recently, Lefkowitz and co-workers reported the discovery of an intracellular small molecule-like allosteric modulator for the β_2-adrenergic receptor (β_2AR) using a combinatorial approach with DNA encoded libraries.[4] The allosteric ligand was found to bind to the intracellular surface of the receptor and inhibit both G protein and arrestin mediated signalling. Kobilka and co-workers crystallised a closely related analogue of the same ligand in complex with the β_2AR-T4 lysozyme fusion protein with the orthosteric inverse agonist carazolol bound. The structure (PDB 5X7D) clearly shows the ligand occupying the G protein binding pocket.[5]

Based on recent bio-structural data of active state GPCRs in complex with GPCR interacting proteins (GIP)[6,7] or mimics thereof[8–12] we wondered if it would be possible to rationally

[a]*Department of Drug Design and Pharmacology, University of Copenhagen, Jagtvej 162, 2100 Copenhagen, Denmark. E-mail: jmm@sund.ku.dk; daniel.pedersen@sund.ku.dk*
[b]*Structural Biology and NMR Laboratory, Department of Biology, University of Copenhagen, Ole Maaløes Vej 5, 2200 Copenhagen, Denmark*
[c]*Department of Neuroscience, University of Copenhagen, Blegdamsvej 3, 2200 Copenhagen, Denmark*

† Electronic supplementary information (ESI) available. See DOI: 10.1039/c7ra11713b

‡ These authors contributed equally as principal investigators.

design peptidomimetics that target the GIP interface. Such allosteric ligands could be beneficial for stabilisation of GPCRs in various conformational states for structural studies, as pharmacological tool compounds, and could possibly provide a new avenue for therapeutic molecules. There have been some reports in the literature on using proteinogenic peptides as GPCR ligands. Hamm and co-workers have published several papers describing that peptides derived from the C-terminus of various G protein α subunits (Gα) are capable of reducing cAMP accumulation by blocking G protein coupling.[13–15] Moreover, Scheerer *et al.* have reported the X-ray crystal structure of rhodopsin in complex with an 11-mer C-terminal peptide from the G_t protein.[10] More recently, we reported our efforts to develop a peptidomimetic that mimics the function of nanobody 80 (Nb80) a well-known allosteric modulator of the β_2AR that binds at the same site of the receptor as the native G_s protein.[9,16]

Using the X-ray crystal structure of the β_2AR in complex with the G_s protein (β_2AR-G_s) as a template (PDB 3SN6)[7] we embarked on a project to identify such allosteric modulators for the β_2AR by a structure-based design approach.

Results and discussion

Peptidomimetic design

Hamm and co-workers previously reported that a peptide comprised of the last 12 amino acid residues from the $G\alpha_s$ C-terminus ($G\alpha_sCT_{12}$) was capable of inhibiting G_s protein coupling to the β_2AR and increased agonist affinity for the receptor.[15] However, in our hands the corresponding proteinogenic 15-mer peptide ($G\alpha_sCT_{15}$) did not block agonist induced cAMP formation in β_2AR cell membranes, whereas Nb80 significantly inhibited the maximal efficacy of ISO (Fig. 1c). Whereas Hamm and co-workers used saponin-permeabilised C6 glioma cells, all peptides reported herein were evaluated in HEK293 membranes overexpressing the β_2AR.[17] We selected to work in a cell membrane-based assay setup to render the intracellular surface freely accessible to the ligands and eliminate issues related to cell permeability. Likewise, Rasmussen

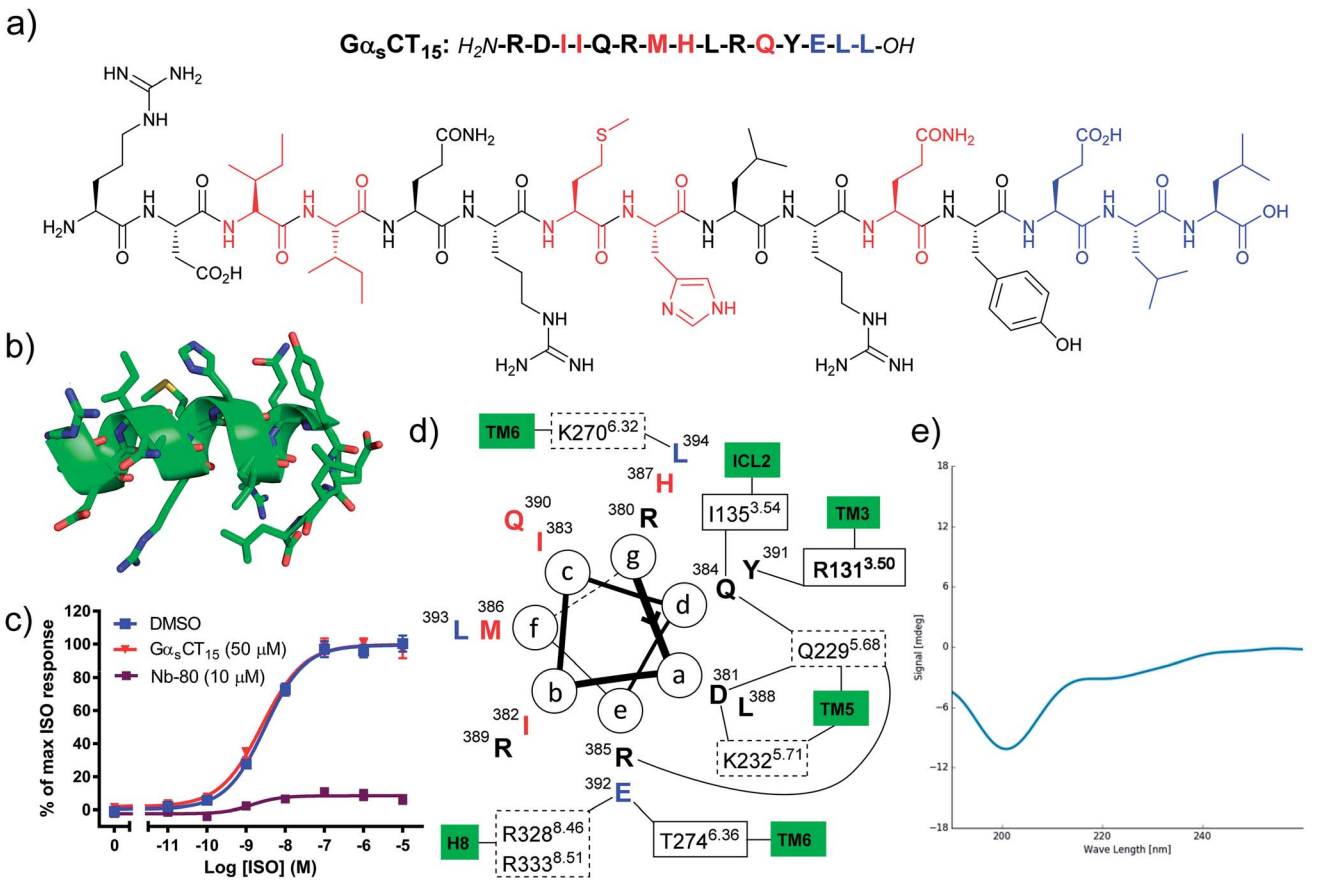

Fig. 1 (a) The native $G\alpha_sCT_{15}$ peptide sequences. Red: residues with no or weak receptor contacts. Blue: reverse turn, not helical, (b) the structure of $G\alpha_sCT_{15}$ extracted from PDB entry 3SN6, (c) the $G\alpha_sCT_{15}$ peptide does not inhibit agonist induced cAMP formation of the β_2AR. Isoproterenol (ISO) concentration–response curves of cAMP accumulation were generated in the absence and presence of 50 μM peptide using HEK293 cell membranes overexpressing the β_2AR. Data represents mean ± SEM from 3–4 independent experiments carried out in duplicates. The known β_2AR-interacting nanobody 80 (Nb80) was included for comparison at 10 μM.[9] (d) Helical wheel projection showing important contacts determined by MD simulation[26] and X-ray crystallography.[7] Dashed boxes: polar contacts involving side chains, solid boxes: polar contacts involving backbone carbonyls, bold box: cation–π interaction, (e) CD spectrum of $G\alpha_sCT_{15}$ indicating a random coil structure (at 50 μM in 10 mM NaH_2PO_4 buffer, pH 6.0).

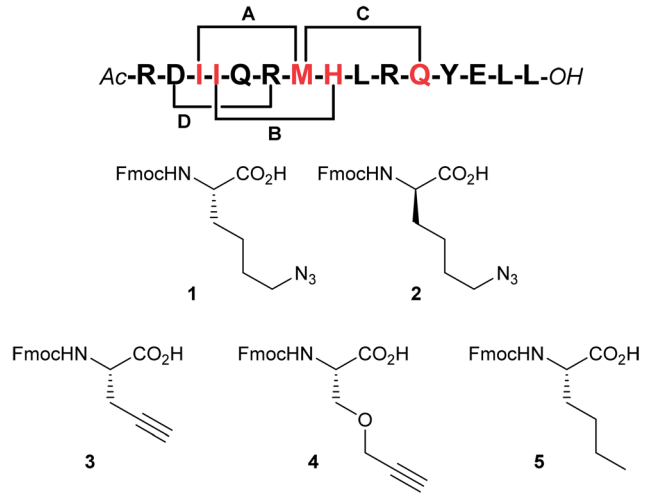

Fig. 2 Stapling positions and unnatural amino acid building blocks. According to our analysis the red residues represent the best (*i*, *i* + 4)-stapling positions by appropriate substitution with amino acids **1**–**4** (staples **A**–**C**). Staple position **D** was included to validate the design (a negative control). To circumvent oxidation problems the norleucine building block **5** was employed as a substitute for methionine (stapling positions **B** and **D**).

et al. were not able to observe any effect of the 20-mer $G\alpha_sCT_{20}$ peptide on β_2AR receptor function and complex formation with β_2AR.[7] However, when $G\alpha_sCT_{20}$ was fused to the carboxy terminus of the β_2AR and expressed as a fusion protein a 27-fold increase in agonist affinity was observed. Based on the results by Rasmussen *et al.* we speculate that $G\alpha_sCT_{20}$ mainly adopts a random coil structure in solution rendering binding to the receptor less favourable. This is consistent with our circular dichroism (CD) analysis of $G\alpha_sCT_{15}$ that showed a random coil structure (Fig. 1e). Also, the affinity of a linear $G\alpha_sCT$ peptide for β_2AR is likely significantly lower than the full G_s protein complex, which has several additional contacts with the receptor. Based on these observations, we hypothesised that it would be necessary to chemically modify the native $G\alpha_sCT_{15}$ peptide to improve binding to the β_2AR. In the β_2AR-G_s X-ray crystal structure the C-terminus of G_s adopts an α-helix terminated by a 3-residue reverse turn (Fig. 1b).[7] Thus, we set out to chemically modify $G\alpha_sCT_{15}$ to pre-organise the peptide in a similar conformation. Peptide stapling is a commonly applied technique for the synthesis of helical peptides.[18–20] Among the many available methods for peptide stapling we favour CuAAC-stapling between amino acids with azido- and alkynyl-modified side chains.[21,22] This methodology was originally developed by Tornoe *et al.*[23] and later optimised by

Table 1 Synthesis of linear and stapled peptidomimetics. Linear peptides were synthesised on 2-chlorotritylresin preloaded with leucine. The N-termini of all peptides were acylated. Peptides **6D**–**9D** were poorly soluble in a variety of solvent systems and were not purified/stapled. The remaining purified (or crude) linear peptides were stapled by CuAAC and purified by preparative RP-HPLC

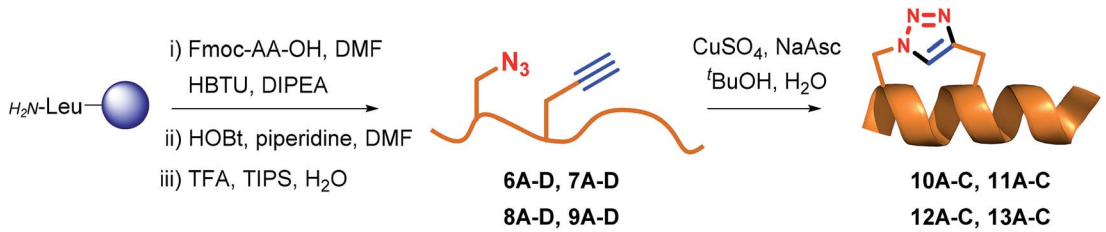

Linear	Amino acid sequence	Stapled	Yield[a]/NPC[b] (%)	Reaction time
$G\alpha_sCT_{15}$	*H*-R-D-I-I-Q-R-M-H-L-R-Q-Y-E-L-L-*OH*	NA	NA	NA
6A	*Ac*-R-D-**1**-I-Q-R-**3**-H-L-R-Q-Y-E-L-L-*OH*	**10A**	36[c]/84	15 min
6B	*Ac*-R-D-I-**1**-Q-R-**5**-**3**-L-R-Q-Y-E-L-L-*OH*	**10B**	10[d]/63	Overnight[e]
6C	*Ac*-R-D-I-I-Q-R-**1**-H-L-R-**3**-Y-E-L-L-*OH*	**10C**	10[d]/45	3 h
6D	*Ac*-R-**1**-I-I-Q-**3**-**5**-H-L-R-Q-Y-E-L-L-*OH*	NA	NA	NA
7A	*Ac*-R-D-**2**-I-Q-R-**3**-H-L-R-Q-Y-E-L-L-*OH*	**11A**	56[c]/77	15 min
7B	*Ac*-R-D-I-**2**-Q-R-**5**-**3**-L-R-Q-Y-E-L-L-*OH*	**11B**	11[d]/72	Overnight[e]
7C	*Ac*-R-D-I-I-Q-R-**2**-H-L-R-**3**-Y-E-L-L-*OH*	**11C**	26[d]/71	1 h
7D	*Ac*-R-**2**-I-I-Q-**3**-**5**-H-L-R-Q-Y-E-L-L-*OH*	NA	NA	NA
8A	*Ac*-R-D-**1**-I-Q-R-**4**-H-L-R-Q-Y-E-L-L-*OH*	**12A**	69[c]/60	1 h
8B	*Ac*-R-D-I-**1**-Q-R-**5**-**4**-L-R-Q-Y-E-L-L-*OH*	**12B**	15[d]/74	1 h
8C	*Ac*-R-D-I-I-Q-R-**1**-H-L-R-**4**-Y-E-L-L-*OH*	**12C**	14[d]/53	2 h
8D	*Ac*-R-**1**-I-I-Q-**4**-**5**-H-L-R-Q-Y-E-L-L-*OH*	NA	NA	NA
9A	*Ac*-R-D-**2**-I-Q-R-**4**-H-L-R-Q-Y-E-L-L-*OH*	**13A**	40[c]/67	Overnight[e]
9B	*Ac*-R-D-I-**2**-Q-R-**5**-**4**-L-R-Q-Y-E-L-L-*OH*	**13B**	13[d]/77	Overnight[e]
9C	*Ac*-R-D-I-I-Q-R-**2**-H-L-R-**4**-Y-E-L-L-*OH*	**13C**	11[d]/60	3 h
9D	*Ac*-R-**2**-I-I-Q-**4**-**5**-H-L-R-Q-Y-E-L-L-*OH*	NA	NA	NA

[a] Yield after preparative HPLC purification to >95% purity (non-NPC corrected). [b] Net peptide content (NPC) (mass% of peptide, the remainder being constituted by counter ions and water). Determined by qNMR (see ESI for details). [c] Synthesised from pure linear peptide. [d] Synthesised from crude linear peptide. Overall yield based on resin loading. [e] Presumably finished in <3 hours but left overnight for practical reasons.

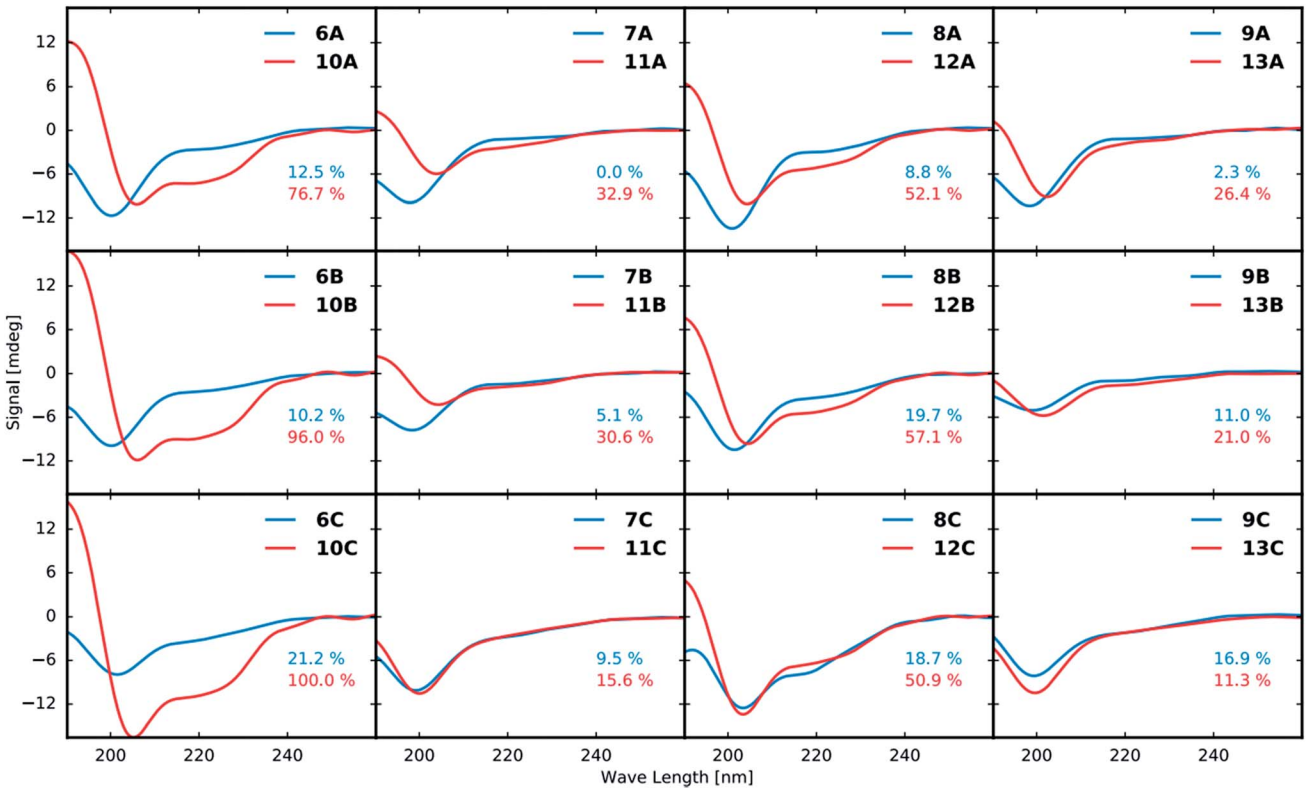

Fig. 3 CD spectra of linear (blue curves) and corresponding stapled (red curves) peptidomimetics at a concentration of 50 μM (10 mM NaH_2PO_4 buffer, pH 6.0). The first row compares stapling at position **A** (Fig. 2), the second row shows stapling position **B** and the third row shows a comparison of stapling position **C**. The columns show a comparison of the different combinations of stapling residues **1** + **3**, **2** + **3**, **1** + **4** and **2** + **4**, respectively. The helicity of the most helical peptidomimetic **10C** as determined by the induced minima at 222 nm and maxima at 190 nm was set to 100% and the helicity of all other peptidomimetics were determined relative to that of **10C**.

Cantel *et al.*[24] and has been applied extensively in (*i*, *i* + 4)-peptide stapling in recent years.[25]

By visual inspection of the β_2AR-G_s X-ray crystal structure we concluded that the 15 C-terminal residues of $G\alpha_s$ participate in important interactions with β_2AR. This is consistent with the conclusions drawn by Hildebrand and co-workers based on MD simulations.[26] In terms of design, it is important that the staple position does not disrupt binding to the target. By visual inspection and based on the MD simulation study by Hildebrand and co-workers 5 residues were identified as potential staple anchoring points (Fig. 1). These 5 residues are ideally positioned for introduction of (*i*, *i* + 4)-staples and four stapling positions would be evaluated in the present study (Fig. 2). Moreover, four different staple designs utilising D- and L-ε-azidolysine (**1–2**), L-propargyl glycine (**3**) and *O*-propargylated L-serine (**4**) would be explored.

Synthesis

Fmoc-protected propargylglycine (**3**) is commercially available and the remaining azide and alkyne modified building blocks were synthesised in house. Azides **1–2** were synthesised from the corresponding Fmoc-protected amines as previously reported[27] using the diazotransfer reagent imidazole sulfonyl azide.[28,29] Alkyne **4** was synthesised in three steps from Boc-protected serine according to the published procedure.[27] Finally, for stapling positions **B** and **D** commercially available norleucine (**5**) was employed as a replacement for the oxidation prone methionine residue.[30] With amino acids **1–5** in hand the linear peptidomimetics **6–9** were synthesised by standard Fmoc-based solid-phase peptide synthesis (SPPS) on chlorotrityl resin and the N-terminus was acylated (Table 1). The synthesis of linear peptides **6–9 A–C** was uneventful and they were all purified by standard preparative RP-HPLC. However, the synthesis of peptides **6D–9D** where two polar residues (D and R) were replaced proved complicated due to poor solubility after cleavage and deprotection. Because peptides **6D–9D** were intended as inactive negative controls we eventually abandoned their purification and stapling due to their poor solubility, which would also translate to problems for pharmacological characterisation. Stapling of purified or crude **6–9 A–C** (see ESI† for details) was carried out in ^{t}BuOH and water (1 : 2 v/v) using $CuSO_4 \cdot 5H_2O$ (1 eq.) and sodium ascorbate (5 eq.) as the *in situ* reducing agent. In general, the CuAAC reaction was clean and went to completion fast (1–3 h) to give stapled peptidomimetics **10–13 A–C** that were purified by preparative RP-HPLC to >95% purity in reasonable yields. Full conversion of linear to stapled peptidomimetic was monitored by RP-HPLC by spiking the reaction sample with the linear starting material, and by FT-IR where the azide stretch (at ~2100 cm^{-1}) is clearly seen to disappear after completion of the stapling reaction (see ESI†).

Table 2 Effect of G_s peptidomimetics on the cAMP accumulation induced by isoproterenol (ISO) at the β_2-adrenergic receptor (β_2AR) in a cell membrane-based cyclic adenosine monophosphate (cAMP) accumulation assay. Basal cAMP level, maximum efficacy, $pEC_{50}(-\log(EC_{50}))$ and Hill slope of the concentration–response curve of ISO in absence and presence of 100 μM peptidomimetic (10 μM for **8C**) were calculated by non-linear regression using GraphPad Prism. Nb80 was tested at 10 μM. Data are given as mean values of *n* number of experiments ± SEM. Significance level $P < 0.05$ (*) calculated by statistical analysis with a one-way ANOVA in GraphPad Prism

Peptide	Basal level	Maximum efficacy	pEC_{50}	Hill slope	*n*
Vehicle	0.0 ± 0.0	100.0 ± 0.0	8.64 ± 0.03	0.81 ± 0.05	6
Nb80	−1.2 ± 0.7	11.3 ± 0.6*	8.98 ± 0.16	0.88 ± 0.29	3
6A	0.7 ± 1.1	90.8 ± 6.0	8.68 ± 0.04	0.81 ± 0.07	3
6B	−2.9 ± 4.2	81.5 ± 4.5	8.48 ± 0.08	0.81 ± 0.12	3
6C	4.6 ± 1.9	89.7 ± 1.5	8.33 ± 0.02	0.83 ± 0.06	3
7A	−0.5 ± 1.5	88.8 ± 8.0	8.74 ± 0.01	0.83 ± 0.10	3
7B	−4.2 ± 1.8	79.9 ± 2.0*	8.58 ± 0.03	0.84 ± 0.04	3
7C	8.4 ± 4.3	88.1 ± 3.6	8.17 ± 0.11	0.87 ± 0.06	3
8A	−1.1 ± 0.7	97.7 ± 5.3	8.67 ± 0.04	0.72 ± 0.02	3
8B	−8.8 ± 2.8	77.1 ± 3.9*	8.46 ± 0.15	0.82 ± 0.07	3
8C	−3.7 ± 2.3	78.0 ± 5.2*	8.65 ± 0.06	0.71 ± 0.07	3
9A	0.4 ± 0.7	92.7 ± 7.5	8.73 ± 0.08	0.83 ± 0.04	3
9B	3.3 ± 4.6	84.1 ± 2.4	7.05 ± 0.38*	0.89 ± 0.05	3
9C	5.7 ± 2.1	88.1 ± 4.5	8.21 ± 0.33	0.92 ± 0.06	3
10A	3.0 ± 0.4	82.8 ± 3.3	8.67 ± 0.05	0.78 ± 0.03	3
10B	−5.0 ± 2.6	80.5 ± 2.2	8.45 ± 0.04	0.72 ± 0.05	3
10C	−11.0 ± 4.3	61.0 ± 4.1*	7.87 ± 0.01	0.63 ± 0.06	3
11A	−1.4 ± 0.7	90.7 ± 4.6	8.53 ± 0.05	0.74 ± 0.03	3
11B	−5.8 ± 3.0	88.0 ± 4.1	8.46 ± 0.07	0.72 ± 0.06	3
11C	−1.9 ± 8.4	78.4 ± 2.6*	8.10 ± 0.12	0.85 ± 0.06	3
12A	0.6 ± 0.4	94.5 ± 6.3	8.68 ± 0.03	0.73 ± 0.04	3
12B	−2.8 ± 4.0	74.0 ± 3.3*	7.87 ± 0.53	0.88 ± 0.09	3
12C	−6.0 ± 2.1	71.7 ± 3.0*	8.52 ± 0.05	0.90 ± 0.06	3
13A	2.4 ± 0.3	90.0 ± 6.4	8.71 ± 0.05	0.85 ± 0.03	3
13B	7.1 ± 5.7	85.1 ± 3.0	7.72 ± 0.30*	0.89 ± 0.04	3
13C	2.3 ± 1.2	82.8 ± 3.8	8.46 ± 0.43	0.80 ± 0.04	3

Structural analysis by circular dichroism (CD)

All purified linear and stapled peptides were subjected to structural analysis by CD. Prior to recording CD spectra, the net peptide content (NPC) for all peptidomimetics was determined by quantitative NMR (qNMR, see ESI†).

The CD data in Fig. 3 shows that stapling in general leads to peptidomimetics with a more helical structure when compared to the linear counterparts. However, the magnitude of the induced helicity varies significantly. While the position of the staple (**A**, **B** or **C**, Fig. 2) does not have a significant effect on the induced helicity, the employed amino acid residues (**1**–**4**) that form the staple have a tremendous effect. Employing residues **1** and **3** clearly increases the helicity of the peptide the most at all three stapling positions. The use of residues **1** and **4** likewise shows strong induction of helicity. In contrast, the use of the D-amino acid **2** in combination with either **3** or **4** lowers the helical induction markedly.

Pharmacology

Membrane-based cAMP accumulation assay. Initially, the stapled peptidomimetics (**10**–**13**) and their linear precursors (**6**–**9**) were tested for their ability to modulate β_2AR agonist-induced cAMP formation. To allow the peptidomimetics to interact with the intracellular G protein binding pocket they were tested in a membrane-based cAMP accumulation assay (see ESI†). In this setup stimulation of β_2AR expressing membranes with various concentrations of the agonist (−)-isoproterenol (ISO) increased cAMP formation in a concentration-dependent manner (mean $pEC_{50} = 8.64 \pm 0.03$). To test the effect of the peptidomimetics on the ISO-induced cAMP formation, similar ISO concentration response curves (CRCs) were generated in presence of a constant concentration of peptidomimetic (100 μM, except for **8C**, which was tested at 10 μM due to poor solubility). The cAMP levels in absence of peptidomimetics were normalised to the basal (0%) and maximal efficacy (100%) of ISO in presence of vehicle (DMSO).

All peptidomimetics stapled at position **A** had little to no effect on the maximum efficacy of ISO (Table 2). Several of the peptidomimetics stapled at positions **B** and **C** displayed a small effect on the maximum efficacy of ISO; **7B**, **8B**, **8C** and **11C** all significantly decreased the maximal efficacy to approximately 80% (Table 2 and Fig. 4). Peptidomimetics **12B** and **12C** had a more pronounced effect and inhibited the maximal efficacy to ~73% on average. Finally, peptidomimetic **10C** affected the maximal ISO efficacy the most by lowering ISO maximal efficacy to 61%. With respect to peptidomimetic-induced effects on ISO potency, **9B** and **13B** significantly decreased the potency by 39- and 8-fold, respectively, but not the efficacy of ISO (Fig. 4). No significant effects of the peptidomimetics were observed on the basal cAMP levels or on the Hill-slope of the fitted curves.

To estimate the potency of the most efficacious peptidomimetic **10C**, increasing concentrations of **10C** up to 200 μM, and

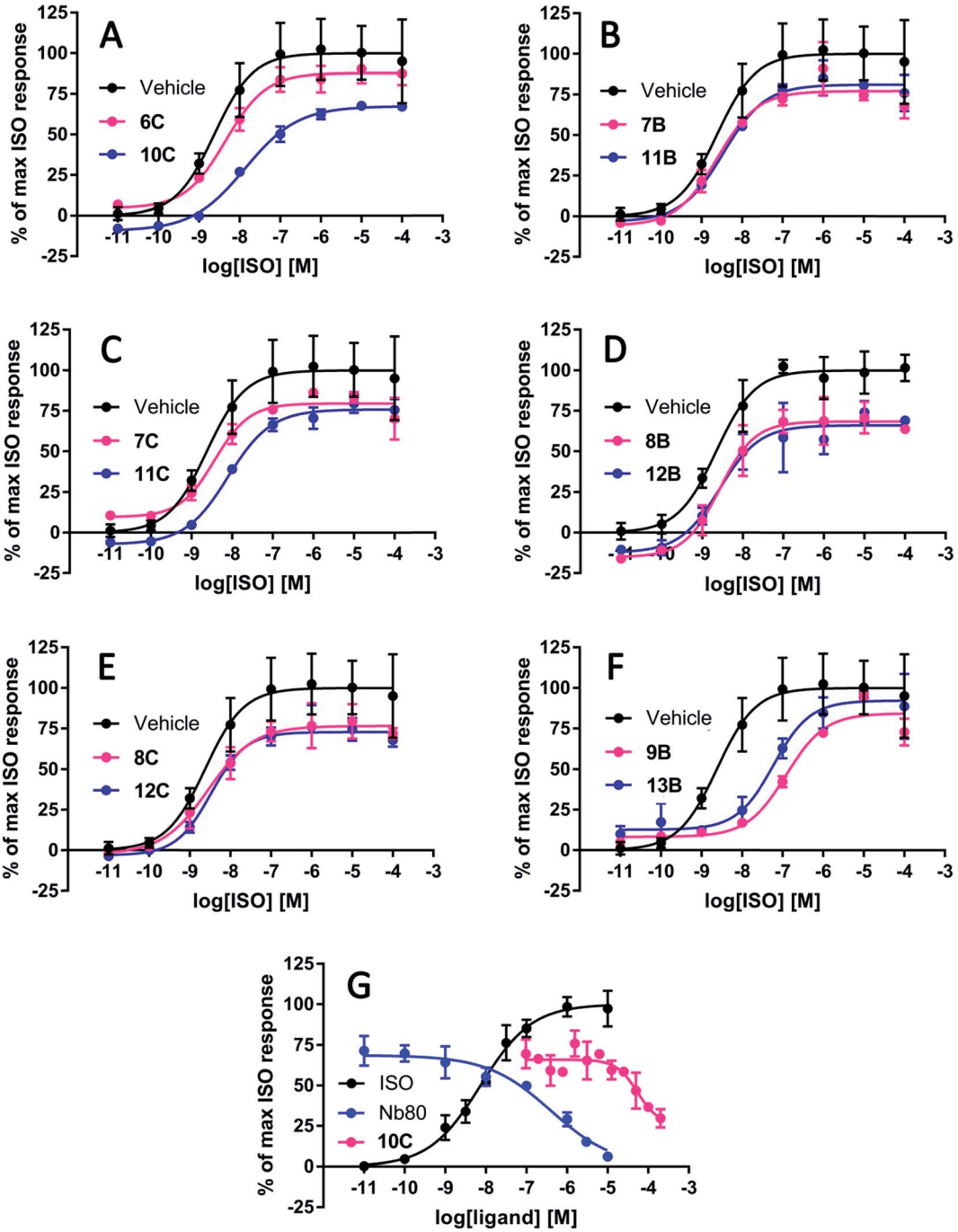

Fig. 4 Representative graphs of the most effective peptidomimetics on the cyclic adenosine monophosphate (cAMP) production induced by the full agonist isoproterenol (ISO) at the β_2-adrenergic receptor (β_2AR). The stapled peptidomimetic **10C** inhibited the maximal response of ISO to 61% whereas its linear precursor **6C** had no significant effect on the ISO-induced cAMP production (A). The linear **7B** (B) and stapled peptidomimetic **11C** (C) inhibited ISO efficacy to a smaller degree (~80%) but significantly. Their stapled (**11B**) and linear counterparts (**7C**) had a minor (~90%) albeit non-statistically significant effects. The linear **8B** and stapled peptidomimetic **12B** pair decreased the maximum response of ISO to 70–80% (D), which is also the case for the linear and stapled pair **8C** and **12C** (E). The linear **9B** and stapled peptidomimetic **13B**, decreased the potency of ISO by 39- and 8-fold, respectively, whereas the efficacy was not affected (F). In presence of ISO corresponding to EC_{75}, the IC_{50} of **10C** was estimated to 55 μM, and the IC_{50} of Nb80 was estimated to 0.40 μM (G).

Nb80 as a control were applied in the presence of an ISO concentration corresponding to EC_{75}. The IC_{50} of **10C** was estimated to 55 μM whereas the IC_{50} of Nb80 was estimated to 0.40 μM (Fig. 4).

Bimane fluorescence shift assay. To further investigate their pharmacological profiles, selected peptidomimetics were tested in a bimane fluorescence shift assay (see ESI†). Labelling of cysteine residue 265 (C265) located in the lower part of the TM6

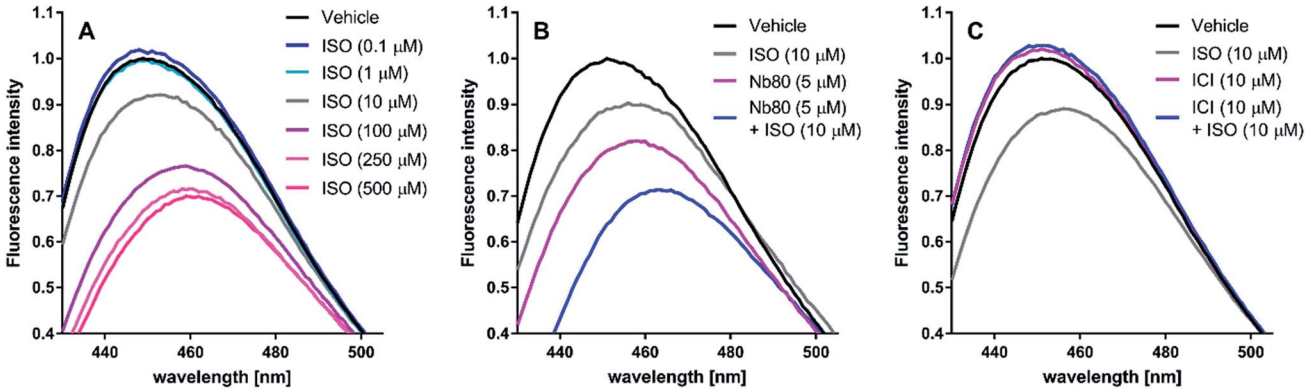

Fig. 5 Representative bimane emission spectra of isoproterenol (ISO), nanobody 80 (Nb80) and ICI-118,551 (ICI) at the β_2-adrenergic receptor (β_2AR). ISO induces an active receptor conformation in a concentration-dependent manner. ISO displays saturating effects at 250 μM and 500 μM (A). Nb80 (5 μM) potentiates the 10 μM ISO-induced bimane-fluorescence response to that of ISO at 250 μM and 500 μM (B). At 10 μM, ICI prevents the receptor activation induced by 10 μM ISO and has a similar effect on the bimane-fluorescence response alone (C).

of β_2AR with a bimane-fluorophore allows detection of conformational changes associated with receptor activation.[31] Stimulation of purified, C265 fluorophore-labelled β_2AR with increasing concentrations of ISO results in a concentration-dependent decrease in the fluorescence intensity (FI) and a red-shift of the maximum emission wavelength (λ_{max}) of the bimane-fluorophore probe (Fig. 5A). The active receptor conformation may be further stabilised in the presence of G protein[31] and G protein mimetics such as Nb80.[9] Indeed, in presence of a partial equilibrium shifting ISO concentration (10 μM), Nb80 is capable of decreasing FI and red-shifting λ_{max} beyond that of ISO (10 μM) or Nb80 (5 μM) alone (Fig. 5B). Conversely, ICI-118,551 (ICI), an inverse agonist capable of stabilising an inactive conformation of β_2AR, blocks the 10 μM ISO-induced response and also slightly increase FI and blue-shifts λ_{max} on its own (Fig. 5C). Thus, the bimane fluorescence shift assay can identify active and inactive-conformation stabilising ligands of the β_2AR.

Based on the results obtained with the cAMP assay, the linear and cyclic peptidomimetic pairs **6C**/**10C**, **7C**/**11C**, **8C**/**12C**, **8B**/**12B** and **9B**/**13B** were tested in the bimane assay at 20 μM (Fig. 6). The peptidomimetics were tested for possible effects on receptor conformation alone and in the presence of 10 μM ISO, which allows detection of peptidomimetic-induced active conformation stabilisation as seen for Nb80. Bimane-fluorescence curves in presence of agonist or peptidomimetic alone or in combination were normalised to that of the receptor alone.

Unlike Nb80, none of the tested peptidomimetic were observed to stabilise an active-like conformation by decreasing FI and red-shifting λ_{max} on their own or by potentiating the response beyond that of 10 μM ISO alone. Although there was a tendency for several peptidomimetics to shift the bimane-fluorescence in the opposite direction (**8B**, **7–8C** and **10–11C**), the peptidomimetics did not affect the response of 10 μM ISO alone. Interestingly, with the exception of peptidomimetic **8B** only the peptidomimetics stapled at position **C** closest to the C-terminal were able to increase FI and blue-shift λ_{max} in a similar way to that seen for the inverse agonist ICI (Fig. 5C).

Discussion

As anticipated CD analysis revealed that the stapled peptidomimetics generally had a higher helical content than their linear counterparts and the native Gα_s 15-mer. The staples comprised of building blocks **1**, **3** and **4** had the highest helical content, whereas the peptidomimetics stapled with D-amino acid **2** and alkynes **3** and **4** contained significantly less helicity. There was no trend regarding the helical content and the stapling positions **A–C**.

The peptidomimetics were evaluated for their ability to block agonist-induced cAMP formation in cell membranes overexpressing the β_2AR. Stapling the peptidomimetics at position **A** was not optimal for blocking cAMP formation by ISO. Thus, both stapled peptidomimetics **12A–13A** and linear peptidomimetics **8A–9A** were essentially inactive, indicating that this stapling position is not ideal for binding to the receptor using the present chemistry. Moving the staple towards the C-terminus (position **B** and **C**) was more favourable. The linear peptidomimetics **7B** and **8B** had a slight, yet significant effect on the maximal ISO response, lowering the efficacy to approximately 80%. Stapled peptidomimetic **12B** had a more pronounced effect on the maximum efficacy with a lowering to 74%. Unexpectedly the **9B**/**13B** pair red-shifted the ISO CRC comparable to that of a competitive antagonist rather than decreasing the maximal agonist efficacy as would be expected for a non-competitive antagonist. The linear **8C** and stapled peptidomimetic **11C** both lowered the maximum efficacy of ISO to approximately 80%. On the other hand, stapled **12C** lowered the efficacy to 72%, whereas stapled **10C** lowered the efficacy to approximately 61%. Thus, **10C** clearly gave the most significant decrease in the maximum efficacy of ISO. In general, the stapled peptidomimetics gave the highest reduction in efficacy and a small tendency for peptidomimetics with a high helical content to have a greater effect was observed (ESI Fig. S1†). Thus, stapled peptidomimetics **10C**, **12B** and **12C** with a relatively high helical content were found to lower the efficacy the most (61–74%). However, the data

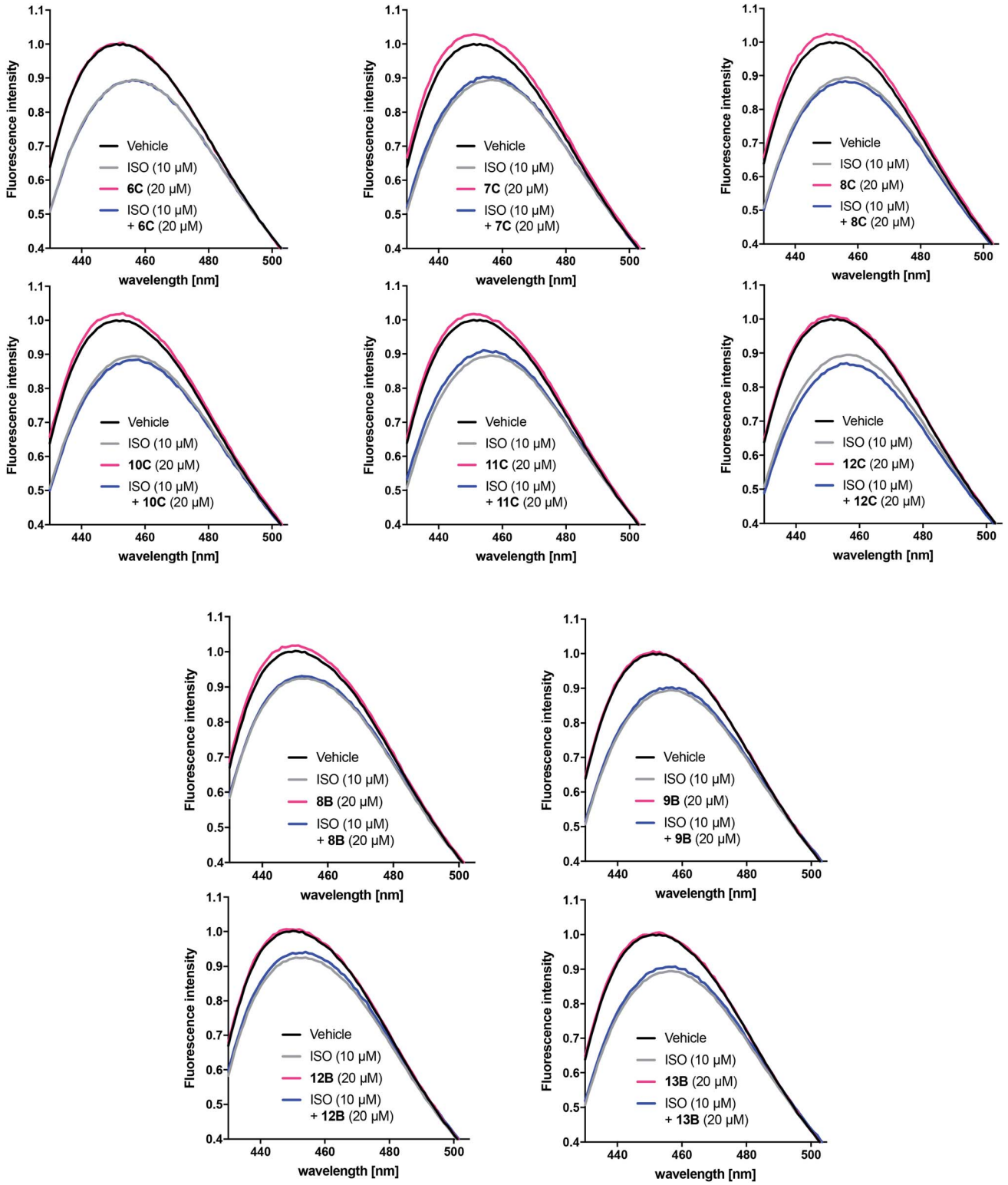

Fig. 6 Representative bimane emission spectra of selected peptidomimetics with significant effects in the cAMP assay. The responses of the linear and cyclic peptidomimetic pairs **6C**/**10C**, **7C**/**11C**, **8C**/**12C**, **8B**/**12B** and **9B**/**13B** were normalised to that of the unliganded β_2AR alone (black solid line). The peptides were tested at 20 μM ($n = 2$ of measurements in triplicate) in the absence (pink solid line) and the presence (blue solid line) of ISO 10 μM (grey solid line).

also shows that a high degree of helicity on its own is not sufficient to give a notable reduction in the formation of cAMP (*e.g.* stapled peptidomimetic **10B**).

When tested in the conformational bimane fluorescence shift assay none of the peptidomimetics stabilised an active-like conformation similar to that of the G protein mimetic Nb80.

However, a small tendency to increase the fluorescence intensity (FI) and blue-shift λ_{max} similar to that for the inverse agonist ICI was seen. The effect was most pronounced for peptidomimetics stapled at position **C** but no correlation between the degree of helicity and the effect on the FI was observed. It cannot be excluded that the concentration tested in the bimane assay was too low to induce a more significant effect.

One interpretation of the obtained pharmacological data is that some of the peptidomimetics (*e.g.* **10C**) are capable of modulating ISO-induced cAMP formation by binding to and thus overlapping with the intracellular binding site of the G protein. However, unlike Nb80, none of the peptidomimetics reported herein stabilise an active-like receptor conformation. Although only small effects of the peptidomimetics were observed it does support the idea of developing intracellular modulators of GPCR signalling derived from hotspot domains of GPCR interacting proteins (*e.g.* the C-termini of G proteins). However, the native C-terminal peptide sequence ($G\alpha_sCT_{15}$) that was employed as a template herein clearly does not provide potent peptidomimetic analogues despite stapling these in a helical conformation. Thus, to render this class of ligands of use for pharmacological and biophysical studies significant optimisation is required. It should be noted that the present study does not provide data that demonstrates that the peptidomimetics are binding in the intended G protein binding pocket. In principle, the peptidomimetics could be engaging the β_2AR elsewhere. Further studies with more potent analogues will be required to determine the mode of action.

Conclusion

In the present study, a series of peptidomimetics that mimic the C-terminal α-helix of the $G\alpha_s$ protein were synthesised as potential allosteric modulators of the β_2AR. The peptidomimetics were characterised pharmacologically in a cAMP accumulation assay and bimane fluorescence assay. Several peptidomimetics inhibited agonist ISO induced cAMP formation by lowering the maximal efficacy of ISO up to 61%. For the most potent peptidomimetic **10C** the IC_{50} for blocking ISO induced cAMP formation was determined to 55 μM. Moreover, some peptidomimetics could decrease the potency of ISO significantly (up to 39-fold). In the bimane fluorescence assay none of the tested peptidomimetics could stabilise an active-like β_2AR conformation. However, we observed a tendency to shift the bimane assay in the opposite direction for some peptidomimetics. Taken together, the data suggests that some of the peptidomimetics can compete with the native G_s protein for the intracellular binding site, but are unable to stabilise an active-like receptor conformation.

To render the peptidomimetics of use as pharmacological tool compounds significant optimisation is required to increase ligand potency. Likewise, to elucidate the mode of action for this class of ligands more potent ligands are required. To this end we are in the process of strengthening ligand–receptor interactions by substitution with natural and unnatural amino acids aided by computational design. The results from these endeavours will be reported elsewhere in due course.

Conflicts of interest

There are no conflicts to declare.

Acknowledgements

The Lundbeck Foundation and the Carlsberg Foundation are gratefully acknowledged for financial support. T. T. P. was supported by the Vietnam International Education Development. M. B. A. K. was supported by a postdoctoral fellowship from the Lundbeck Foundation and K. L. L. was supported by a Hallas-Møller stipend from the Novo Nordisk Foundation. S. G. F. R. was supported by the Lundbeck Foundation (Grant R37-A3457), the Danish Independent Research Council (Grant 0602-02407B), and the UNIK Center for Synthetic Biology.

References

1 J. P. Overington, B. Al-Lazikani and A. L. Hopkins, How many drug targets are there?, *Nat. Rev. Drug Discovery*, 2006, **5**, 993–996.

2 A. S. Hauser, M. Attwood, M. Rask-Andersen, H. B. Schiöth and D. E. Gloriam, Trends in GPCR Drug Discovery – New Targets and Indications, *Nat. Rev. Drug Discovery*, 2017, **16**, 829–842.

3 P. Fronik, B. I. Gaiser and D. S. Pedersen, Bitopic Ligands and Metastable Binding Sites: Opportunities for G Protein-Coupled Receptor (GPCR) Medicinal Chemistry, *J. Med. Chem.*, 2017, **60**, 4126–4134.

4 S. Ahn, A. W. Kahsai, B. Pani, Q. T. Wang, S. Zhao, A. L. Wall, R. T. Strachan, D. P. Staus, L. M. Wingler, L. D. Sun, J. Sinnaeve, M. Choi, T. Cho, T. T. Xu, G. M. Hansen, M. B. Burnett, J. E. Lamerdin, D. L. Bassoni, B. J. Gavino, G. Husemoen, E. K. Olsen, T. Franch, S. Costanzi, X. Chen and R. J. Lefkowitz, Allosteric β-blocker isolated from a DNA-encoded small molecule library, *Proc. Natl. Acad. Sci. U. S. A.*, 2017, **114**, 1708–1713.

5 X. Liu, S. Ahn, A. W. Kahsai, K. C. Meng, N. R. Latorraca, B. Pani, A. J. Venkatakrishnan, A. Masoudi, W. I. Weis, R. O. Dror, X. Chen, R. J. Lefkowitz and B. K. Kobilka, Mechanism of intracellular allosteric β_2AR antagonist revealed by X-ray crystal structure, *Nature*, 2017, **548**, 480–484.

6 Y. Kang, X. E. Zhou, X. Gao, Y. He, W. Liu, A. Ishchenko, A. Barty, T. A. White, O. Yefanov, G. W. Han, Q. Xu, P. W. de Waal, J. Ke, M. H. Tan, C. Zhang, A. Moeller, G. M. West, B. D. Pascal, E. N. Van, L. N. Caro, S. A. Vishnivetskiy, R. J. Lee, K. M. Suino-Powell, X. Gu, K. Pal, J. Ma, X. Zhi, S. Boutet, G. J. Williams, M. Messerschmidt, C. Gati, N. A. Zatsepin, D. Wang, D. James, S. Basu, S. Roy-Chowdhury, C. E. Conrad, J. Coe, H. Liu, S. Lisova, C. Kupitz, I. Grotjohann, R. Fromme, Y. Jiang, M. Tan, H. Yang, J. Li, M. Wang, Z. Zheng, D. Li, N. Howe, Y. Zhao, J. Standfuss, K. Diederichs, Y. Dong, C. S. Potter, B. Carragher, M. Caffrey, H. Jiang, H. N. Chapman, J. C. Spence, P. Fromme, U. Weierstall, O. P. Ernst, V. Katritch, V. V. Gurevich, P. R. Griffin, W. L. Hubbell, R. C. Stevens, V. Cherezov, K. Melcher and

H. E. Xu, Crystal structure of rhodopsin bound to arrestin by femtosecond X-ray laser, *Nature*, 2015, **523**, 561.

7 S. G. F. Rasmussen, B. T. DeVree, Y. Zou, A. C. Kruse, K. Y. Chung, T. S. Kobilka, F. S. Thian, P. S. Chae, E. Pardon, D. Calinski, J. M. Mathiesen, S. T. A. Shah, J. A. Lyons, M. Caffrey, S. H. Gellman, J. Steyaert, G. Skiniotis, W. I. Weis, R. K. Sunahara and B. F. Kobilka, Crystal structure of the β_2 adrenergic receptor-G_s protein complex, *Nature*, 2011, **477**, 549.

8 B. Carpenter, R. Nehmé, T. Warne, A. G. W. Leslie and C. G. Tate, Structure of the adenosine A2A receptor bound to an engineered G protein, *Nature*, 2016, **536**, 104.

9 S. G. F. Rasmussen, H. J. Choi, J. J. Fung, E. Pardon, P. Casarosa, P. S. Chae, B. T. DeVree, D. M. Rosenbaum, F. S. Thian, T. S. Kobilka, A. Schnapp, I. Konetzki, R. K. Sunahara, S. H. Gellman, A. Pautsch, J. Steyaert, W. I. Weis and B. K. Kobilka, Structure of a nanobody-stabilized active state of the β_2 adrenoceptor, *Nature*, 2011, **469**, 175.

10 P. Scheerer, J. H. Park, P. W. Hildebrand, Y. J. Kim, N. Krauss, H. W. Choe, K. P. Hofmann and O. P. Ernst, Crystal structure of opsin in its G-protein-interacting conformation, *Nature*, 2008, **455**, 497.

11 A. K. Shukla, A. Manglik, A. C. Kruse, K. Xiao, R. I. Reis, W. C. Tseng, D. P. Staus, D. Hilger, S. Uysal, L. Y. Huang, M. Paduch, P. Tripathi-Shukla, A. Koide, S. Koide, W. I. Weis, A. A. Kossiakoff, B. K. Kobilka and R. J. Lefkowitz, Structure of active β-arrestin-1 bound to a G-protein-coupled receptor phosphopeptide, *Nature*, 2013, **497**, 137.

12 M. Szczepek, F. Beyrière, K. P. Hofmann, M. Elgeti, R. Kazmin, A. Rose, F. J. Bartl, D. von Stetten, M. Heck, M. E. Sommer, P. W. Hildebrand and P. Scheerer, Crystal structure of a common GPCR-binding interface for G protein and arrestin, *Nat. Commun.*, 2014, **5**, 4801.

13 E. L. Martin, S. Rens-Domiano, P. J. Schatz and H. E. Hamm, Potent peptide analogues of a G protein receptor-binding region obtained with a combinatorial library, *J. Biol. Chem.*, 1996, **271**, 361.

14 M. R. Mazzoni, S. Taddei, L. Giusti, P. Rovero, C. Galoppini, A. D'Ursi, S. Albrizio, A. Triolo, E. Novellino, G. Greco, A. Lucacchini and H. E. Hamm, A galpha(s) carboxyl-terminal peptide prevents G(s) activation by the A(2A) adenosine receptor, *Mol. Pharmacol.*, 2000, **58**, 226.

15 M. M. Rasenick, M. Watanabe, M. B. Lazarevic, S. Hatta and H. E. Hamm, Synthetic peptides as probes for G protein function. carboxyl-terminal G alpha s peptides mimic G_s and evoke high affinity agonist binding to beta-adrenergic receptors, *J. Biol. Chem.*, 1994, **269**, 21519.

16 C. Martin, S. Moors, M. Danielsen, C. Betti, C. Fabris, D. Sejer Pedersen, E. Pardon, M. Peyressatre, K. Fehér, J. C. Martins, J. Mosolff Mathiesen, M. Morris, N. Devoogdt, V. Caveliers, F. De Proft, J. Steyaert and S. Ballet, Rational Design of Nanobody80 Loop Peptidomimetics: Towards Biased β_2 Adrenergic Receptor Ligands, *Chem.–Eur. J.*, 2017, **23**, 9632.

17 J. M. Mathiesen, L. Vedel and H. Bräuner-Osborne, cAMP biosensors applied in molecular pharmacological studies of G protein-coupled receptors, *Methods Enzymol.*, 2013, **522**, 191.

18 T. A. Hill, N. E. Shepherd, F. Diness and D. P. Fairlie, Constraining Cyclic Peptides To Mimic Protein Structure Motifs, *Angew. Chem., Int. Ed.*, 2014, **53**, 13020.

19 Y. H. Lau, P. de Andrade, Y. Wu and D. R. Spring, Peptide stapling techniques based on different macrocyclisation chemistries, *Chem. Soc. Rev.*, 2015, **44**, 91.

20 C. J. White and A. K. Yudin, Contemporary strategies for peptide macrocyclization, *Nat. Chem.*, 2011, **3**(7), 509.

21 P. T. Tran, C. Ø. Larsen, T. Røndbjerg, M. De Foresta, M. B. A. Kunze, A. Marek, J. H. Løper, L.-E. Boyhus, A. Knuhtsen, K. Lindorff-Larsen and D. S. Pedersen, Diversity-Oriented Peptide Stapling: A Third Generation Copper-Catalysed Azide−Alkyne Cycloaddition Stapling and Functionalisation Strategy, *Chem.–Eur. J.*, 2017, **23**, 3490.

22 A. D. Pehere, M. Pietsch, M. Gutschow, P. M. Neilsen, D. S. Pedersen, S. Nguyen, O. Zvarec, M. J. Sykes, D. F. Callen and A. D. Abell, Synthesis and Extended Activity of Triazole-Containing Macrocyclic Protease Inhibitors, *Chem.–Eur. J.*, 2013, **19**, 7975.

23 C. W. Tornoe, C. Christensen and M. Meldal, Peptidotriazoles on solid phase: [1,2,3]-triazoles by regiospecific copper(I)-catalyzed 1,3-dipolar cycloadditions of terminal alkynes to azides, *J. Org. Chem.*, 2002, **67**, 3057.

24 S. Cantel, A. L. C. Isaad, M. Scrima, J. J. Levy, R. D. DiMarchi, P. Rovero, J. A. Halperin, A. M. D'Ursi, A. M. Papini and M. Chorev, Synthesis and conformational analysis of a cyclic peptide obtained *via i* to $i + 4$ intramolecular side-chain to side-chain azide – alkyne 1,3-dipolar cycloaddition, *J. Org. Chem.*, 2008, **73**, 5663.

25 D. S. Pedersen and A. Abell, 1,2,3-Triazoles in Peptidomimetic Chemistry, *Eur. J. Org. Chem.*, 2011, 2399.

26 A. S. Rose, M. Elgeti, U. Zachariae, H. Grubmüller, K. P. Hofmann, P. Scheerer and P. W. Hildebrand, Position of Transmembrane Helix 6 Determines Receptor G Protein Coupling Specificity, *J. Am. Chem. Soc.*, 2014, **136**, 11244–11247.

27 T. J. Sminia and D. S. Pedersen, Azide- and Alkyne-Functionalised α- and β3-Amino Acids, *Synlett*, 2012, **23**, 2643.

28 E. D. Goddard-Borger and R. V. Stick, An Efficient, Inexpensive, and Shelf-Stable Diazotransfer Reagent: Imidazole-1-sulfonyl Azide Hydrochloride, *Org. Lett.*, 2007, **9**, 3797.

29 H. Johansson and D. S. Pedersen, Azide- and Alkyne-Derivatised α-Amino Acids, *Eur. J. Org. Chem.*, 2012, 4267.

30 A. M. Gilles, P. Marlière, T. Rose, R. Sarfati, R. Longin, A. Meier, S. Fermandjian, M. Monnot, G. N. Cohen and O. Bârzu, Conservative replacement of methionine by norleucine in Escherichia coli adenylate kinase, *J. Biol. Chem.*, 1988, **263**, 8204.

31 X. J. Yao, G. Vélez-Ruiz, M. R. Whorton, S. G. F. Rasmussen, B. T. DeVree, X. Deupi, R. K. Sunahara and B. Kobilka, The effect of ligand efficacy on the formation and stability of a GPCR-G protein complex, *Proc. Natl. Acad. Sci. U. S. A.*, 2009, **106**, 9501.

